Synthesis, Structure, and Ligand Redistribution Equilibria of Mixed Ligand Complexes of the Heavier Group 2 Elements Containing Pyrazolato and β-Diketiminato Ligands

Hani M. El-Kaderi,[a] Mary Jane Heeg,[a] and Charles H. Winter*[a]

Keywords: N ligands / Group 2 elements / Calcium / Strontium / Barium

Treatment of $M[N(SiMe_3)_2]_2(THF)_2$ (M = Ca, Sr, Ba) with various stoichiometries of *N*-*tert*-butyl-4-(*tert*-butylimino)-2-penten-2-amine ($L^{tBu}H$) and 3,5-di-*tert*-butylpyrazole (tBu_2pzH) afforded $[(\eta^2\text{-}tBu_2pz)Ca(\mu\text{-}\eta^5{:}\eta^2\text{-}tBu_2pz)(\mu\text{-}\eta^2{:}\eta^2\text{-}tBu_2pz)Ca(\eta^5\text{-}L^{tBu})]$ (17 %), $[Sr(\mu\text{-}\eta^5{:}\eta^2\text{-}tBu_2pz)(\eta^5\text{-}L^{tBu})]_2$ (50 %), and $[Ba(\mu\text{-}\eta^5{:}\eta^2\text{-}tBu_2pz)(\eta^5\text{-}L^{tBu})]_2$ (66 %) as colorless crystalline solids. The formulations of the new complexes were assigned from spectral and analytical data and by X-ray crystal structure determinations. In the solid state, $[(\eta^2\text{-}tBu_2pz)Ca(\mu\text{-}\eta^5{:}\eta^2\text{-}tBu_2pz)(\mu\text{-}\eta^2{:}\eta^2\text{-}tBu_2pz)Ca(\eta^5\text{-}L^{tBu})]$ exists as a dimer that is held together by $\mu\text{-}\eta^5{:}\eta^2$- and $\mu\text{-}\eta^2{:}\eta^2$-pyrazolato ligands, with a terminal $\eta^2\text{-}tBu_2pz$ ligand on one calcium ion and an $\eta^5\text{-}L^{tBu}$ ligand on the other. The dimeric structures of $[Sr(\mu\text{-}\eta^5{:}\eta^2\text{-}tBu_2pz)(\eta^5\text{-}L^{tBu})]_2$ and $[Ba(\mu\text{-}\eta^5{:}\eta^2\text{-}tBu_2pz)(\eta^5\text{-}L^{tBu})]_2$ are connected by two $\mu\text{-}\eta^5{:}\eta^2$-pyrazolato ligands, and the coordination sphere of each metal ion is capped with an $\eta^5\text{-}L^{tBu}$ ligand. In toluene solution, $[(\eta^2\text{-}tBu_2pz)Ca(\mu\text{-}\eta^5{:}\eta^2\text{-}tBu_2pz)(\mu\text{-}\eta^2{:}\eta^2\text{-}tBu_2pz)Ca(\eta^5\text{-}L^{tBu})]$ exists as an equilibrium mixture of at least four compounds. In toluene solution, $[Sr(\mu\text{-}\eta^5{:}\eta^2\text{-}tBu_2pz)(\eta^5\text{-}L^{tBu})]_2$ exists in equilibrium with $Sr(\eta^5\text{-}L^{tBu})_2$ and $Sr_4(tBu_2pz)_8$. A van't Hoff analysis of this equilibrium between 46 and 104 °C afforded $\Delta H° = 22.2 \pm 0.7$ kcal/mol, $\Delta S° = 43.7 \pm 1.9$ cal/mol·K, and $\Delta G°(298\ K) = 9.2 \pm 0.9$ kcal/mol. $[Ba(\mu\text{-}\eta^5{:}\eta^2\text{-}tBu_2pz)(\eta^5\text{-}L^{tBu})]_2$ exists in toluene solution as a single, pure species between –60 and +80 °C. The overall results suggest that the $\eta^5\text{-}L^{tBu}$ ligand is better at saturating the coordination sphere of the metal ion to which it coordinates than is the tBu_2pz ligand, and is suggested as a more promising ligand for the construction of practical, volatile chemical vapor deposition film growth precursors.

Introduction

Recent efforts in the coordination chemistry of calcium, strontium, and barium have been driven by applications in polymerization catalysis, organic synthesis, and film growth by chemical vapor deposition (CVD) and related techniques.[1–5] Solid state materials containing the group 2 elements have many significant technological applications, and CVD is commonly used for the growth of thin films of these materials.[1–3] Despite intense investigation, CVD precursors of the heavier group 2 elements remain problematic.[1–3] It has been difficult to identify structures that combine sufficient volatility and thermal stability, due to the high molecular weights, the high coordination numbers, and the low formation constants of complexes containing these elements. The key to future developments in this area must reside with ligand design. To date, the most widely used group 2 CVD precursors have employed substituted cyclopentadienyl[2] or β-diketonato[3] ligands.

Our laboratory has devoted considerable effort to the development of new nitrogen-based pyrazolato[6] and β-diketiminato[7] ligands for the group 2 elements. In particular, we have found that group 2 bis(pyrazolato) complexes form monomers only in the presence of neutral donor ligands, but these complexes decompose prior to sublimation with loss of the neutral ligands to afford oligomeric pyrazolato complexes with very low vapor pressures.[6] We have also recently reported that β-diketiminato ligands with alkyl substituents on the nitrogen atoms bond to group 2 metal centers with π- or η^5-coordination modes, and that these ligands coordinate unexpectedly well to the larger group 2 metal ions.[7] Herein we describe a surprising series of dimeric calcium, strontium, and barium complexes that contain both β-diketiminato and pyrazolato ligands. The β-diketiminato ligands coordinate to the metal centers with a terminal η^5-coordination mode, while the pyrazolato ligands adopt terminal η^2-, $\mu\text{-}\eta^2{:}\eta^2$-, or $\mu\text{-}\eta^5{:}\eta^2$-coordination modes. Documentation of pyrazolato ligand coordination modes has been a central theme of many research reports in recent years,[8] but there have been few reports of heavier group 2 pyrazolato complexes.[6b,9] The results described herein afford unusual examples of pyrazolato ligand coordination to group 2 centers, provide a conceptual method for

[a] Department of Chemistry, Wayne State University, Detroit, Michigan 48202, USA
Fax: +1-313-577-8289
E-mail: chw@chem.wayne.edu

Supporting information for this article is available on the WWW under http://www.eurjic.org or from the author.

reduction of oligomerization in pyrazolato complexes through inclusion of terminal η^5-β-diketiminato ligands, allow direct comparison of the donor characteristics of β-diketiminato and pyrazolato ligands, and suggest new directions for the development of ligands that can be used to manipulate the properties of group 2 complexes. We also describe ligand redistribution equilibria of the new heteroleptic complexes and provide thermodynamic parameters for the $[Sr(\mu\text{-}\eta^5\text{:}\eta^2\text{-}t\text{Bu}_2\text{pz})(\eta^5\text{-L}^{t\text{Bu}})]_2$ equilibria.

Results

Synthetic Chemistry

Treatment of $M[N(SiMe_3)_2]_2(THF)_2$ (M = Ca, Sr, Ba)[10] with various stoichiometries of *N*-*tert*-butyl-4-(*tert*-butylimino)-2-penten-2-amine ($L^{t\text{Bu}}H$)[11] and 3,5-di-*tert*-butylpyrazole ($t\text{Bu}_2\text{pzH}$) as described in Equation (1) afforded $[(\eta^2\text{-}t\text{Bu}_2\text{pz})\text{Ca}(\mu\text{-}\eta^5\text{:}\eta^2\text{-}t\text{Bu}_2\text{pz})(\mu\text{-}\eta^2\text{:}\eta^2\text{-}t\text{Bu}_2\text{pz})\text{Ca}(\eta^5\text{-L}^{t\text{Bu}})]$ (**1**, 17%), $[Sr(\mu\text{-}\eta^5\text{:}\eta^2\text{-}t\text{Bu}_2\text{pz})(\eta^5\text{-L}^{t\text{Bu}})]_2$ (**2**, 50%), and $[Ba(\mu\text{-}\eta^5\text{:}\eta^2\text{-}t\text{Bu}_2\text{pz})(\eta^5\text{-L}^{t\text{Bu}})]_2$ (**3**, 66%) as colorless crystalline solids. Variations in the $L^{t\text{Bu}}H/t\text{Bu}_2\text{pzH}$ stoichiometries away from those required for **1** did not lead to new products, and only **1** crystallized from the reaction mixtures. Interestingly, the highest crystallized yields of **1** were obtained with an $L^{t\text{Bu}}H/t\text{Bu}_2\text{pzH}$ ratio of 2:2 and not 1:3 as required for the stoichiometry of **1**. The order of reagent addition was important in the synthesis of **1**–**3**. If $t\text{Bu}_2\text{pzH}$ was added first, followed by $L^{t\text{Bu}}H$, then complex product mixtures resulted. Complex **1** is soluble in hexane, while **2** and **3** are insoluble in hexane and are moderately soluble in toluene at room temperature. The structural assignments for **1**–**3** were based upon spectral and analytical data as well as X-ray structure determinations. In solution, **1** exists as an equilibrium mixture of at least four species at ambient temperature, while **2** exists as an equilibrium mixture of three species. By contrast, **3** is a single species in solution between –60 and +80 °C. The variable-temperature NMR spectroscopic data for these complexes are described below.

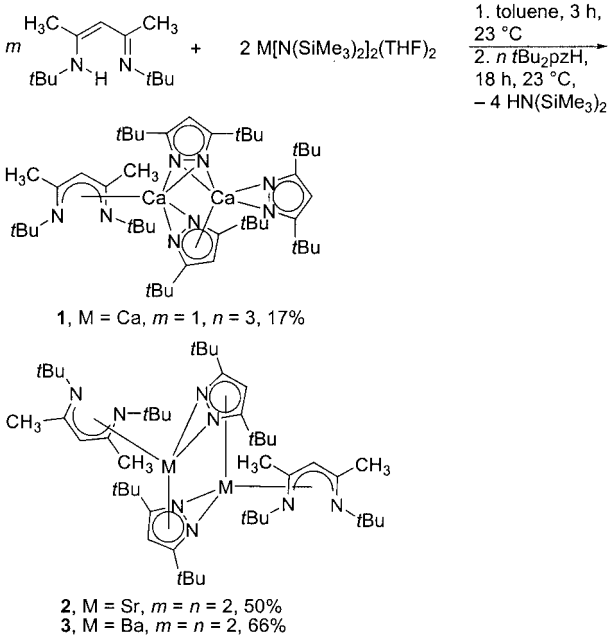

(1)

X-ray Crystal Structure Determinations

The crystal structures of **1**–**3** were determined in order to understand their molecular structures. Perspective views of **1**–**3** are shown in Figures 1, 2 and 3. The crystal data are given in Table 1. Selected bond lengths and angles are presented in Tables 2, 3 and 4.

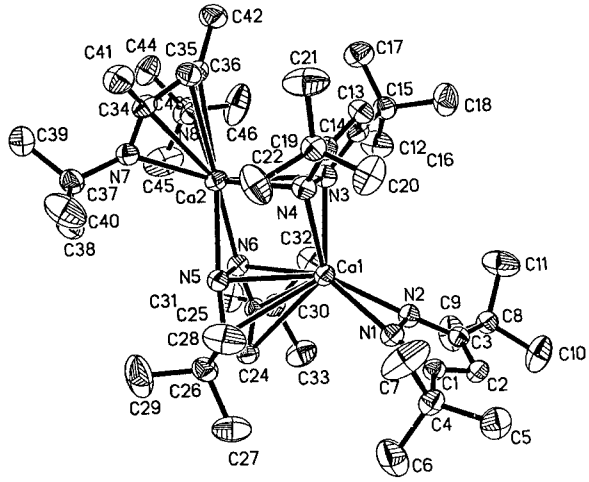

Figure 1. Perspective view of **1** with thermal ellipsoids at the 50% probability level.

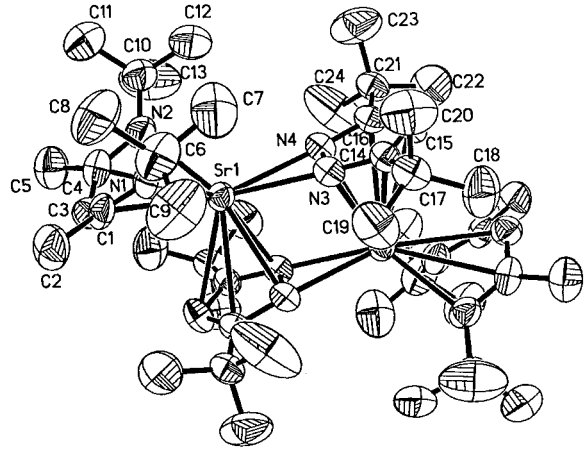

Figure 2. Perspective view of **2** with thermal ellipsoids at the 50% probability level.

In the solid state, **1** can be thought of as $Ca(\eta^5\text{-L}^{t\text{Bu}})(\eta^2\text{-}t\text{Bu}_2\text{pz})$ and $Ca(\eta^2\text{-}t\text{Bu}_2\text{pz})_2$ fragments that dimerize through formation of $\mu\text{-}\eta^5\text{:}\eta^2$- and $\mu\text{-}\eta^2\text{:}\eta^2$-pyrazolato ligands (Figure 1). The $\eta^5\text{-L}^{t\text{Bu}}$ ligand has calcium–nitrogen bond lengths of 2.322(2) and 2.342(2) Å, while the calcium–carbon bond lengths range between 2.741(3) and 2.827(3) Å. These values are slightly shorter than those observed in $Ca(\eta^5\text{-L}^{t\text{Bu}})_2$ (Ca–N 2.342–2.358, Ca–C 2.817–2.901 Å).[7b] The terminal η^2-pyrazolato ligand has cal-

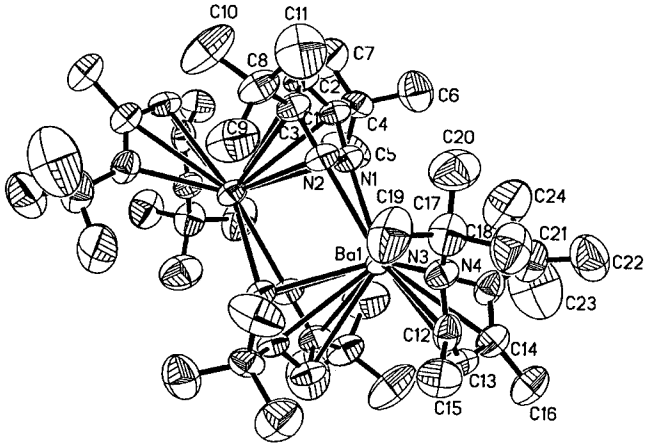

Figure 3. Perspective view of **3** with thermal ellipsoids at the 50% probability level.

Table 1. Summary of crystallographic data for **1**–**3**.

	1	**2**	**3**
Empirical formula	$C_{46}H_{82}Ca_2N_8$	$C_{48}H_{88}N_8Sr_2$	$C_{48}H_{88}Ba_2N_8$
Formula mass	827.36	952.50	1051.94
Temperature [K]	193(2)	295(2)	295(2)
Crystal system	monoclinic	monoclinic	triclinic
Space group	*P*21/*c*	*P*21/*n*	$P\bar{1}$
a [Å]	10.6303(8)	14.609(14)	10.6553(13)
b [Å]	20.8169(15)	12.343(16)	11.4231(15)
c [Å]	22.6456(17)	15.596(18)	12.1090(16)
α [°]	90	90	78.097(2)
β [°]	91.643(2)	101.61(3)	74.841(3)
γ [°]	90	90	83.296(3)
V [Å^{-3}]	5009.2(6)	2755(6)	1388.9(3)
Z	4	2	1
d(calcd.) [g/cm^3]	1.097	1.148	1.258
Absorption coefficient [mm^{-1}]	0.265	1.972	1.445
F(000)	1816	1016	544
Crystal size [mm]	0.30×0.20×0.10	0.20×0.20×0.05	0.12×0.12×0.06
θ range [°]	1.92 to 28.31	1.74 to 28.28	2.30 to 28.32
No. of reflections collected	26303	19680	9890
No. of independent reflections	11683	6410	6393
GOF/F^2	0.998	0.750	0.974
R indices [$I > 2\sigma(I)$]	0.0493	0.0460	0.0637
R indices (all data)	0.1233	0.2021	0.1649
Largest difference peak/hole [e·Å^{-3}]	0.305, –0.339	0.389, –0.599	0.637, –0.833

$R(F) = \Sigma||F_o| - |F_c||/\Sigma|F_o|$; $Rw(F) = [\Sigma w(F_o^2 - F_c^2)^2/\Sigma w(F_o^2)^2]^{1/2}$

Table 2. Selected bond lengths [Å] and angles [°] for **1**.

Ca(1)–N(1) 2.3154(19)	Ca(1)–C(23) 2.832(2)
Ca(1)–N(2) 2.299(2)	Ca(1)–C(24) 2.997(2)
Ca(1)–N(3) 2.438(2)	Ca(1)–C(25) 2.863(2)
Ca(1)–N(4) 2.433(2)	Ca(2)–C(34) 2.773(2)
Ca(1)–N(5) 2.583(2)	Ca(2)–C(35) 2.741(3)
Ca(1)–N(6) 2.5984(19)	Ca(2)–C(36) 2.827(3)
Ca(2)–N(3) 2.642(2)	Ca(1)–Ca(2) 3.5348(7)
Ca(2)–N(4) 2.588(2)	N(1)–Ca(1)–N(2) 35.29(6)
Ca(2)–N(5) 2.480(2)	N(3)–Ca(1)–N(4) 33.74(6)
Ca(2)–N(6) 2.452(2)	N(5)–Ca(1)–N(6) 31.26(6)
Ca(2)–N(7) 2.322(2)	N(5)–Ca(2)–N(6) 32.88(6)
Ca(2)–N(8) 2.342(2)	N(3)–Ca(2)–N(4) 31.35(6)
N(7)–Ca(2)–N(8) 77.87(7)	

Table 3. Selected Bond lengths [Å] and angles [°] for 2.[a]

Sr–N(1) 2.516(5)	Sr–C(15)′ 3.229(5)
Sr–N(2) 2.512(4)	Sr–C(16)′ 3.083(5)
Sr–N(3) 2.618(4)	Sr–Sr′ 4.097(2)
Sr–N(4) 2.614(5)	N(1)–Sr–N(2) 71.95(14)
Sr–N(3)′ 2.897(4)	N(3)–Sr–N(4) 31.15(10)
Sr–N(4)′ 2.855(4)	N(3)′-Sr–N(4)′ 28.26(9)
Sr–C(1) 3.052(6)	N(2)–Sr–N(4) 109.27(17)
Sr–C(3) 3.004(6)	N(1)–Sr–N(4) 127.11(14)
Sr–C(4) 3.025(6)	N(2)–Sr–N(3) 129.79(14)
Sr–C(14)′ 3.148(5)	N(1)–Sr–N(3) 106.43(15)

[a] Primes indicate symmetry-equivalent positions.

Table 4. Selected bond lengths [Å] and angles [°] for **3**.[a]

Ba–N(1) 2.776(6)	Ba–C(3)′ 3.241(8)
Ba–N(2) 2.793(6)	Ba–Ba′ 4.297(2)
Ba–N(3) 2.642(6)	N(1)–Ba–N(2) 28.99(16)
Ba–N(4) 2.633(6)	N(1)–Ba–N(3) 123.49(19)
Ba–N(1)′ 3.004(6)	N(1)–Ba–N(4) 115.4(2)
Ba–N(2)′ 3.036(6)	N(2)–Ba–N(3) 104.98(19)
Ba–C(12) 3.121(8)	N(2)–Ba–N(4) 133.5(2)
Ba–C(13) 3.110(8)	N(3)–Ba–N(4) 67.98(19)
Ba–C(14) 3.176(8)	N(1)′-Ba–N(2)′ 26.67(15)
Ba–C(1)′ 3.189(8)	N(1)′-Ba–N(3) 128.00(18)
Ba–C(2)′ 3.325(8)	N(1)′-Ba–N(4) 144.0(2)

[a] Primes indicate symmetry-equivalent positions

cium–nitrogen bond lengths of 2.315(2) and 2.299(2) Å, which can be compared to the corresponding values in complexes of the formula Ca(η^2-$R_2pz)_2$L (R = Me, *t*Bu;L = neutral donor; Ca–N = 2.311–2.529 Å).[6b] The calcium–nitrogen bond lengths for the μ-η^2:η^2-*t*Bu_2pz ligand are 2.438(2) and 2.433(2) Å for Ca(1) and 2.588(2) and 2.642(2) Å for Ca(2). Thus, the μ-η^2:η^2-*t*Bu_2pz ligand is more strongly bonded to Ca(1), and this metal center is assigned as the Ca(η^2-*t*Bu_2pz)$_2$ fragment. For Ca(2), the calcium–nitrogen bond lengths for the μ-η^5:η^2-*t*Bu_2pz ligand are 2.452(2) and 2.480(2) Å, while for Ca(1) these values are 2.583(2) and 2.598(2) Å. The calcium–carbon bond lengths range from 2.832(2) to 2.997(2) Å. Based upon bond lengths, Ca(2) is more strongly bonded to the pyrazolato ligand containing N(5) and N(6), and thus Ca(2) is assigned as the Ca(η^5-L$^{t\mathrm{Bu}}$)(η^2-*t*Bu_2pz) fragment. The Ca(1)–carbon(pyrazolato) distances are longer than the Ca(2)–C(η^5-L$^{t\mathrm{Bu}}$) distances in **1**, and are comparable to those observed in Ca(η^5-L$^{t\mathrm{Bu}}$)$_2$.[7b] The calcium–carbon bond length in Ca($C_5Me_5)_2$ is 2.64(2) Å.[12] Thus, the η^5-pyrazolato ligand interaction involving Ca(1) within **1** is best described as a π-donor interaction and is different from the terminal η^5-pyrazolato ligand bonding that has been described in several ruthenium complexes.[13]

The overall molecular structures of **2** and **3** are similar, and can be viewed as dimers of two M(η^5-L$^{t\mathrm{Bu}}$)(η^2-*t*Bu_2pz) fragments (Figures 2 and 3). The η^5-L$^{t\mathrm{Bu}}$ ligand in **2** has strontium–nitrogen bond lengths of 2.512(4) and 2.516(5) Å, while the strontium–carbon bond lengths range between 3.004(6) and 3.052(6) Å. The analogous barium–nitrogen distances in **3** are 2.633(6) and 2.642(6) Å, while the barium–carbon distances range between 3.110(8) and 3.176(8) Å. The values are comparable to those of Sr(η^5-

$L^{tBu})_2$ [Sr–N 2.473(2)–2.517(2) Å, Sr–C 2.928(2)–3.004(2) Å] and Ba(η^5-L^{tBu})$_2$ (Ba–N 2.617–2.680 Å, Ba–C 3.055–3.157 Å).[7b] The metal–carbon distances in **2** and **3** are slightly longer than the metal–carbon distances in Sr[C_5(tBu)$_3H_2$]$_2$(THF) (Sr–$C_{Cp'}$ 2.87 Å avg.)[14] and Ba(C_5Me_5)$_2$ [2.98(1), 2.99(2) Å].[12] The μ-η^5:η^2-tBu$_2$pz ligand in **2** possesses strontium–nitrogen bond lengths of 2.614(5) and 2.618(5) Å for the η^2-interaction, and 2.855(4) and 2.897(4) Å for the η^5-bonded fragment. For **3**, the related values are 2.776(6) and 2.793(6) Å for the η^2-interaction, and 3.004(6) and 3.036(6) Å for the η^5-bonded fragment. The metal–carbon distances associated with the μ-η^5:η^2-tBu$_2$pz ligand range between 3.083(5) and 3.229(5) Å for **2** and 3.189(8)–3.325(8) Å for **3**. These values are similar to or longer than those associated with the η^5-L^{tBu} ligand in **2** and **3** and M(η^5-L^{tBu})$_2$,[7b] and are 5–10% longer than the related distances in Sr[C_5(tBu)$_3H_2$]$_2$(THF) (Sr–$C_{Cp'}$ 2.87 Å avg.)[14] and Ba(C_5Me_5)$_2$ [2.98(1), 2.99(2) Å].[12] Again, the bond lengths associated with the μ-η^5:η^2-tBu$_2$pz ligand suggest that the η^5-interactions are best described as π-donation to satisfy the Lewis acidity of the unsaturated metal centers. The angle between the planes of the β-diketiminato and pyrazolato C_3N_2 cores is 20.8(3)° in **2** and 23.5(3)° in **3**, which can be compared with C_5Me_5(centroid)–metal–C_5Me_5(centroid) angles of 26–33° in the monomeric, base-free metallocenes M(C_5Me_5)$_2$.[12]

Variable-Temperature NMR Behavior of 1–3

Having established the solid-state structures, we next explored the solution structures using NMR spectroscopy. The solution NMR behavior of **1**–**3** differed significantly. Complex **1** exhibited four β-diketiminato ligand β-CH ^{1}H NMR resonances in [D_8]toluene at ambient temperature at δ = 4.60, 4.44, 4.22, and 4.20 ppm, in a ratio of 26:15:12:47. The resonance at δ = 4.22 ppm was identified as the β-CH resonance of Ca(η^5-L^{tBu})$_2$, by comparison with authentic material {also δ = 1.98 (CH_3), 1.34 [C(CH_3)$_3$] ppm}.[7b] Thus, Ca(η^5-L^{tBu})$_2$ is a minor constituent of the solution. A species with resonances consistent with **1** was observed in the ^{1}H NMR spectrum {δ = 6.19, 6.08, 6.04 (tBu$_2$pz β-CH), 4.20 (L^{tBu} β-CH), 1.96 (L^{tBu} CH_3), 1.45, 1.40, 1.28 [L^{tBu} C(CH_3)$_3$]}, and accounted for 47% of the integrated β-CH signals. The remaining two β-diketiminato ligand L^{tBu} β-CH resonances correspond to unknown species, but probably contain mixed pyrazolato/L^{tBu} ligand spheres. The complex Ca$_3$(tBu$_2$Pz)$_6$ has been recently described,[9d] and has tBu$_2$pz β-CH resonances at δ = 6.20, 6.08, and 6.00 ppm and a *tert*-butyl methyl resonance at δ = 1.37 ppm in the ^{1}H NMR in [D_8]toluene at –55 °C. In the ^{1}H NMR spectrum of **1** in [D_8]toluene at –60 °C, tBu$_2$pz β-CH resonances were observed at δ = 6.34, 6.29, 6.23, 6.18, and 6.08 ppm. These resonances do not match those reported for Ca$_3$(tBu$_2$pz)$_6$. It is possible that Ca$_3$(tBu$_2$pz)$_6$ precipitates from [D_8]toluene at –60 °C, and is thus not observed. The presence of **1**, Ca(η^5-L^{tBu})$_2$, and one or two other unidentified species in solutions derived from pure **1** suggest that multiple equilibria are present.

In [D_8]toluene at ambient temperature, **2** exhibited a mixture of two complexes containing β-diketiminato ligands [δ = 4.21, 4.19 (L^{tBu} β-CH) ppm] in a 13:87 ratio. The major species exhibits the resonances expected for **2** {δ = 6.26 (tBu$_2$pz β-CH), 4.19 (L^{tBu} β-CH), 1.99 (L^{tBu} CH_3), 1.47, 1.30 [L^{tBu}, tBu$_2$pz C(CH_3)$_3$]}. The minor species matches the resonances that we have previously reported for Sr(η^5-L^{tBu})$_2$.[7b] The presence of Sr(η^5-L^{tBu})$_2$ suggests the equilibrium depicted in Equation (2), wherein **2** converts partially in [D_8]toluene to Sr(η^5-L^{tBu})$_2$ and the recently reported tetramer Sr$_4$(tBu$_2$pz)$_8$.[9d] The ^{1}H NMR spectrum of **2** at –60 °C in [D_8]toluene revealed 1:1:1 pyrazolato β-CH resonances at δ = 6.35, 6.26, and 6.07 ppm and a *tert*-butyl methyl resonance at δ = 1.44 ppm, after the resonances for Sr(η^5-L^{tBu})$_2$ and **2** had been excluded. For comparison, the ^{1}H NMR spectrum of Sr$_4$(tBu$_2$pz)$_8$ at –60 °C in [D_8]toluene is reported to have pyrazolato β-CH resonances at δ = 6.31, 6.16, and 6.08 ppm and a *tert*-butyl methyl resonance at δ = 1.48 ppm.[9d] Thus, our ^{1}H NMR spectrum at –60 °C supports the presence of Sr$_4$(tBu$_2$pz)$_8$ in the equilibrium mixture. Below 46 °C, the mixture of Sr(η^5-L^{tBu})$_2$ and **2** remained approximately constant, possibly due to a kinetically slow approach to the equilibrium. Above 46 °C, however, the Sr(η^5-L^{tBu})$_2$/**2** ratio increased with temperature (Table 5). Accordingly, we carried out a van't Hoff analysis of the equilibrium depicted in Equation (2). The equilibrium constants shown in Table 2 were determined between 46 and 104 °C by integration of the β-diketonate β-CH resonances of Sr(η^5-L^{tBu})$_2$ and **2**, and then calculating the concentrations of each species. The concentration of Sr$_4$(tBu$_2$pz)$_8$ could not be measured directly between 46 and 104 °C due to very broad signals,[9d] but was calculated at each temperature by assuming a stoichiometry of 1:4 with Sr(η^5-L^{tBu})$_2$. Analysis of the data for the equilibrium depicted in Equation (2) using standard procedures for van't Hoff analyses[15] afforded $\Delta H°$ = 22.2 ± 0.7 kcal/mol, $\Delta S°$ = 43.7 ± 1.9 cal/mol·K, and $\Delta G°$(298 K) = 9.2 ± 0.9 kcal/mol. Consistent with an equilibrium process possessing a positive $\Delta G°$, the equilibrium at 298 K lies strongly toward **2** and is reflected by the small K_{eq} values in Table 2.

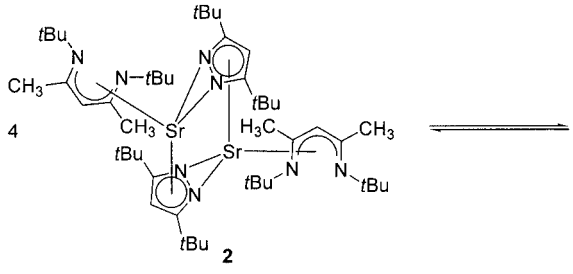

K_{eq} = [Sr(η^5-L^{tBu})$_2$]^4[Sr$_4$(tBu$_2$pz)$_8$]/[**2**]^4 (2)

Table 5. Equilibrium constants for **2** at various temperatures.

T [K]	K_{eq} [M]
319.2	2.17×10^{-6}
323.7	3.20×10^{-6}
328.1	5.26×10^{-6}
332.6	8.60×10^{-6}
337.0	1.39×10^{-5}
341.5	2.54×10^{-5}
345.6	4.52×10^{-5}
350.2	6.66×10^{-5}
354.4	9.74×10^{-5}
358.3	1.19×10^{-4}
363.8	1.41×10^{-4}
368.2	1.93×10^{-4}
372.7	3.29×10^{-4}
377.2	4.40×10^{-4}

In contrast to **1** and **2**, the ^{1}H NMR spectra of **3** between –60 and +80 °C in [D$_8$]toluene revealed a single species with resonances consistent with the solid-state structure. Thus, **3** shows no evidence for equilibria similar to those described for **1** and **2**.

Discussion

The η^5-coordination of the diketiminato ligands is a prominent structural feature of **1**–**3**. We have recently reported that complexes of the formula M(η^5-L$^{t\mathrm{Bu}}$)$_2$ (M = Ca, Sr, Ba) adopt sandwich-like structures with η^5-L$^{t\mathrm{Bu}}$ ligands.[7] In our paper on M(η^5-L$^{t\mathrm{Bu}}$)$_2$,[7b] we analyzed the η^5-L$^{t\mathrm{Bu}}$ bonding in terms of the planes incorporating the atoms MN$_2$ (a), N$_2$(C$_\alpha$)$_2$ (b), and (C$_\alpha$)$_2$C$_\beta$ (c). For M(η^5-L$^{t\mathrm{Bu}}$)$_2$, the a/b angles were between 70 and 72° and the b/c angles were between 25 and 26°, and these metrical parameters were used to support the η^5-coordination mode and differentiate it from the more common η^2-form (which has much smaller a/b and b/c values[7]). The corresponding metrical parameters for **1**–**3** are as follows: **1**: a/b = 74.9° and b/c = 29.4°; **2**: a/b = 70.5° and b/c = 29.0°; **3**: a/b = 70.5° and b/c = 28.7°. These values are close to those of M(η^5-L$^{t\mathrm{Bu}}$)$_2$, and are consistent with similar η^5-bonding of the L$^{t\mathrm{Bu}}$ ligands in **1**–**3**. All of the other heavier group 2 β-diketiminato complexes described to date feature 2,6-diisopropylphenyl,[4d,5,16] 2-methoxyphenyl,[17] or cyclohexyl[18] moieties as the nitrogen substituents. Calcium, strontium, and barium complexes containing the 2,6-diisopropylphenyl-substituted ligand [CH{C(CH$_3$)N(2,6-*i*Pr$_2$C$_6$H$_3$)}$_2$]$^-$ (L$^{\mathrm{Ar}}$) exhibit the η^2-coordination mode, through the nitrogen atoms of L$^{\mathrm{Ar}}$. Use of the *N*-cyclohexyl-substituted diketiminato ligand [CH{C(CH$_3$)N(C$_6$H$_{11}$)}$_2$]$^-$ (L$^{\mathrm{Cy}}$) afforded the dimeric barium complex Ba$_2$(L$^{\mathrm{Cy}}$)$_3$[N(SiMe$_3$)$_2$], which contains η^5-, μ-η^2:η^2:η^5-, and μ-η^2:η^3-β-diketiminato ligands.[18] Adoption of the η^2-coordination mode in complexes containing L$^{\mathrm{Ar}}$ is presumably a steric effect that is driven by the bulky aromatic isopropyl substituents. The various coordination modes of β-diketiminato ligands have been recently reviewed.[19] The η^5-β-diketiminato ligand has been structurally documented in a few main group, lanthanide, and early transition metal complexes, but still remains rare.[7b,18,19] The present results, our previous report on M(η^5-L$^{t\mathrm{Bu}}$)$_2$,[7b] and Ba$_2$(L$^{\mathrm{Cy}}$)$_3$[N(SiMe$_3$)$_2$][18] suggest that the η^5-β-diketiminato coordination mode should be common in the heavier group 2 complexes when alkyl groups or less bulky aromatic rings are present on the nitrogen atoms.

Complex **1** contains terminal η^2-, μ-η^5:η^2-, and μ-η^2:η^2-pyrazolato ligands, while **2** and **3** possess μ-η^5:η^2-pyrazolato ligands. The terminal η^2-coordination mode has been documented in Ca(R$_2$pz)$_2$(L$_n$) (L$_n$ = polydentate oxygen or nitrogen donor),[6b] M(Ph$_2$pz)$_2$(THF)$_4$ (M = Ca, Sr, Ba),[9c] M(Ph$_2$pz)$_2$(DME)$_n$ (M = Ca, Sr, *n* = 2; M = Ba, *n* = 3),[9c] M(Me$_2$pz)$_2$(Me$_2$pzH)$_4$ (M = Ca, Sr),[9c] Ca$_3$(*t*Bu$_2$pz)$_6$,[9d] Sr$_4$(*t*Bu$_2$pz)$_8$,[9d] and Ba$_6$(*t*Bu$_2$pz)$_{12}$.[9d] Terminal η^2-pyrazolato ligands are thus common in the heavier group 2 metal complexes, and are probably driven by achieving maximum electrostatic interactions between the pyrazolato ligand in-plane nitrogen-based orbitals and the group 2 metal ions. One pyrazolato ligand in **1** adopts the μ-η^2:η^2-coordination mode. This coordination mode has been previously observed in Ca$_3$(*t*Bu$_2$pz)$_6$[9d] and in lanthanide complexes such as Ln$_3$(Ph$_2$pz)$_9$ (Ln = La, Nd).[21] The similar ionic radii[22] of Ca$^{\mathrm{II}}$ (1.00 Å), La$^{\mathrm{III}}$ (1.032 Å), and Nd$^{\mathrm{III}}$ (0.983 Å) are most likely the origin of the similar pyrazolato ligand coordination modes. Finally, **1**–**3** contain μ-η^5:η^2-pyrazolato ligands. This coordination mode has been previously observed in the group 2 complexes Ca$_3$(*t*Bu$_2$pz)$_6$,[9d] Sr$_4$(*t*Bu$_2$pz)$_8$,[9d] and Ba$_6$(*t*Bu$_2$pz)$_{12}$,[9d] and in lanthanide complexes such as Ln$_3$(Ph$_2$pz)$_9$ (Ln = La, Nd)[21] and Eu$_4$(*t*Bu$_2$pz)$_8$.[23] Formation of μ-η^5:η^2-pyrazolato ligands appears to arise due to the coordinative unsaturation at the group 2 and lanthanide metal ions, which can be satisfied in the absence of good neutral donor ligands by donation of the out-of-plane π-orbitals of the pyrazolato ligand C$_3$N$_2$ cores to an adjacent metal ion. In **1**–**3**, the μ-η^5:η^2-pyrazolato ligands lead to dimeric species, whereas in the other group 2 and lanthanide complexes, trimers, tetramers, and even hexamers are obtained through formation of μ-η^5:η^2-pyrazolato ligands. It is clear that the good donor capabilities of L$^{t\mathrm{Bu}}$ restrict the degree of oligomerization in **1**–**3**.

The overall structures of **1**–**3** can be compared with those of Ca$_3$(*t*Bu$_2$pz)$_6$,[9d] Sr$_4$(*t*Bu$_2$pz)$_8$,[9d] Ba$_6$(*t*Bu$_2$pz)$_{12}$,[9d] and Eu$_4$(*t*Bu$_2$pz)$_8$.[23] Table 6 compares selected metal–nitrogen bond lengths in **1**–**3** with the related fragments in Ca$_3$(*t*Bu$_2$pz)$_6$,[9d] Sr$_4$(*t*Bu$_2$pz)$_8$,[9d] and Ba$_6$(*t*Bu$_2$pz)$_{12}$.[9d] Remarkably, the Ca$_2$(η^2-*t*Bu$_2$pz)(μ-η^5:η^2-*t*Bu$_2$pz)(μ-η^2:η^2-*t*Bu$_2$pz) fragment in **1** is virtually identical structurally to the coordination sphere of the outer and middle calcium ions in Ca$_3$(*t*Bu$_2$pz)$_6$. Indeed, if an outer Ca(*t*Bu$_2$pz)$_3^-$ fragment in Ca$_3$(*t*Bu$_2$pz)$_6$ is replaced by L$^{t\mathrm{Bu}}$, the molecular structure of **1** is obtained. Such similarity suggests that the Ca$_2$(η^2-*t*Bu$_2$pz)(μ-η^5:η^2-*t*Bu$_2$pz)(μ-η^2:η^2-*t*Bu$_2$pz) fragment is particularly stable. The structural parameters of the M$_2$(μ-η^5:η^2-*t*Bu$_2$pz)$_2$ core fragments in **2** and **3** show a similar high degree of congruence with the inner metal ion M$_2$(μ-η^5:η^2-*t*Bu$_2$pz)$_2$ substructures of Sr$_4$(*t*Bu$_2$pz)$_8$, Ba$_6$(*t*Bu$_2$pz)$_{12}$, and Eu$_4$(*t*Bu$_2$pz)$_8$. In fact, as shown in Table 6, the metal–nitrogen bond lengths of the M$_2$(μ-η^5:η^2-*t*Bu$_2$pz)$_2$ substructures in **2** and Sr$_4$(*t*Bu$_2$pz)$_8$ and **3** and Ba$_6$(*t*Bu$_2$-

Table 6. Comparison of pyrazolato metal–nitrogen distances in **1**–**3** with those of $Ca_3(tBu_2pz)_6$, $Sr_4(tBu_2pz)_8$, and $Ba_6(tBu_2pz)_{12}$.

Complex	M–N [Å] terminal η^2	M–N [Å] μ-η^2:η^2	M–N [Å] μ-η^5:η^2	M–C [Å] μ-η^5:η^2
1	2.299(2)	2.433(2)	2.452(2)	2.832(2)
	2.315(2)	2.438(2)	2.480(2)	2.997(2)
		2.588(2)	2.583(2) (π)	2.863(2)
		2.642(2)	2.598(2) (π)	
$Ca_3(tBu_2pz)_6$[9d]	2.303(3)	2.447(4)–2.618(4)	2.415(3)–2.455(3)	2.816(5)–2.960(4)
[Ca(1) and Ca(2) only]	2.318(3)		2.577(3)–2.583(3) (π)	
2			2.614(5)	3.083(5)
			2.618(4)	3.229(5)
			2.855(4) (π)	3.148(5)
			2.897(4) (π)	
$Sr_4(tBu_2pz)_8$[9d]			2.453(9)–2.648(6)	3.029(7)–3.381(9)
[Sr(1) and Sr(2) only]			2.730(6)–2.779(6) (π)	
3			2.776(6)	3.189(8)
			2.793(6)	3.325(8)
			3.004(6) (π)	3.241(8)
			3.036(6) (π)	
$Ba_6(tBu_2pz)_{12}$[9d]			2.72(1)–2.84(1)	3.10(1)–3.39(1)
[Ba(1) and Ba(2) only]			2.89(1)–3.06(1) (π)	

$pz)_{12}$ are very similar. Replacement of the outer two $Sr(tBu_2pz)_3^-$ fragments in $Sr_4(tBu_2pz)_8$ by L^{tBu} ligands affords the molecular structure of **2**. In $Ba_6(tBu_2pz)_{12}$, replacement of outer $Ba(tBu_2pz)_3^-$ and $Ba_3(tBu_2pz)_7^-$ fragments by two L^{tBu} ligands affords the molecular structure of **3**. Such close structural similarities suggest that the $M_2(\mu\text{-}\eta^5\text{:}\eta^2\text{-}tBu_2pz)_2$ substructure is particularly stable, and that this unit is likely to be observed in other strontium and barium complexes that contain tBu_2pz ligands. As in **1**, the L^{tBu} ligands in **2** and **3** are sterically saturating and block these complexes from forming higher oligomeric structures.

The redistribution equilibria of **1**–**3** are of relevance to recent reports of lactide polymerization catalysis by unsymmetrical group 2 complexes (LMX) containing β-diketiminato ligands (L).[4e,16,17] In such catalysis, it is presumably the unsymmetrical LMX complex that is the active and desired precatalyst, since X^- possesses the needed nucleophilic properties to initiate catalysis and the steric properties of L are designed to promote stereoselectivity in the polymerizations. By contrast, ML_2 is unlikely to initiate catalysis efficiently and MX_2 may not promote stereoselective polymerization. A recent report by Hill has explored the stability of β-diketiminato complexes of the formula $L^{Ar}M[N(SiMe_3)_2](THF)$ toward ligand redistribution in solution.[16a] Interestingly, $L^{Ar}Ca[N(SiMe_3)_2](THF)$ was found to be inert toward ligand redistribution in [D_8]toluene solution at ambient temperature, while $L^{Ar}Ba[N(SiMe_3)_2](THF)$ was in equilibrium with $Ba(L^{Ar})_2$ and $Ba[N(SiMe_3)_2](THF)_x$ under the same conditions. Thermodynamic parameters were not reported for the latter system. It was proposed that the larger size and lower Lewis acidity of the barium ion makes it more susceptible toward ligand redistribution, compared to $L^{Ar}Ca[N(SiMe_3)_2](THF)$.[16a] The equilibrium trend observed for $L^{Ar}M[N(SiMe_3)_2](THF)$ is the opposite of what we have observed in the present study. Qualitatively, **1** undergoes more ligand redistribution at ambient temperature than **2**, since the percentage of the dimeric starting material present in **1** (47%) is lower than in **2** (87%). Thus, the order of ligand redistribution in solution is **1** > **2** >> **3**. While it was not possible to carry out a van't Hoff analysis on **1**, due to the multiple equilibria, the thermodynamic parameters for **2** provide some insight into the factors that stabilize the heteroleptic structures for **1**–**3**. In view of the positive $\Delta G°$ values for **2** in the temperature range that was studied (46–104 °C), the K_{eq} values are very small and strongly favor the heteroleptic starting material. In **2**, $\Delta H°$ is large (22.2 ± 0.3 kcal/mol), but this value is offset by a large $\Delta S°$ value (43.7 ± 0.3 cal/mol·K), which allows the ΔG° values to decrease and the K_{eq} values to increase with increasing temperature. We have previously proposed that the L^{tBu} ligands in $M(\eta^5\text{-}L^{tBu})_2$ bond most strongly to the barium ion and least strongly to the calcium ion, based upon comparison of the metal–nitrogen and metal–carbon bond lengths with those of Cp^*_2M.[7b] If this proposal holds for **1**–**3**, then the $\Delta H°$ values should increase in the order **1** < **2** < **3**, which follows the qualitative trend in redistribution equilibria. It is also likely that there is an entropic contribution to the equilibria, since the homoleptic pyrazolato complexes adopt the oligomeric structures $Ca_3(tBu_2pz)_6$, $Sr_4(tBu_2pz)_8$, and $Ba_6(tBu_2pz)_{12}$ in the solid state and appear to adopt similar structures in solution.[9d] Thus, the $\Delta S°$ values should decrease in the order **1** > **2** > **3** to reflect the increasing organization required for the oligomeric series. It is likely that the resistance of **3** toward ligand exchange in solution results from a combination of optimum bonding to the L^{tBu} ligands and the entropic penalty associated with the formation of the hexameric product $Ba_6(tBu_2pz)_{12}$. These results suggest that the nature of the ligands has a pronounced effect upon redistribution equilibria of heteroleptic group 2 complexes, and that appropriate choice of ligands can reverse the normal redistribution equilibrium trend of Ca > Sr > Ba.[16a] There are few other equilibrium constant data with which those of **2** can be compared. Cp*CaI(THF)$_2$ is

reported to dissociate in [D$_8$]THF to afford Cp*$_2$Ca(THF)$_2$ and CaI$_2$(THF)$_2$ with K_{eq} = 4.[24] (C$_5$*i*Pr$_4$H)CaI(OEt$_2$)$_n$ dissociates in diethyl ether to Ca(C$_5$*i*Pr$_4$H)$_2$ and CaI$_2$(OEt$_2$)$_n$ with an estimated K_{eq} of 2.[25] Mixtures of Ba(CH$_2$C$_6$H$_5$)$_2$(THF)$_2$ and Ba(C$_5$Me$_4$SiMe$_2$C$_6$H$_5$)$_2$ favor the heteroleptic complex Ba(C$_5$Me$_4$SiMe$_2$C$_6$H$_5$)(CH$_2$C$_6$H$_5$)(THF) with K_{eq} values that are much greater than one.[26] The complex [Ba(C$_5$H*i*Pr$_4$)(I)(THF)$_2$]$_2$ resists ligand redistribution in tetrahydrofuran, but does scramble ligands in less coordinating solvents such as benzene.[27] Redistribution equilibria are also important for the heavier group 2 Grignard analogs.[28]

With regards to the design of heavier group 2 metal complexes for thin film growth applications, our previous study of M(η^5-L$^{t\mathrm{Bu}}$)$_2$[7b] and the results herein demonstrate that the L$^{t\mathrm{Bu}}$ ligand is very effective at blocking a face of the metal ion to which it coordinates toward further oligomerization. By contrast, the *t*Bu$_2$pz ligand does not provide the same degree of steric saturation as the L$^{t\mathrm{Bu}}$ ligand, which leads to oligomeric complexes containing various pyrazolato ligand coordination modes in the absence of neutral amine or ether donor ligands. While Ca$_3$(*t*Bu$_2$pz)$_6$, Sr$_4$(*t*Bu$_2$pz)$_8$, and Ba$_6$(*t*Bu$_2$pz)$_{12}$ are reported to be volatile,[9d] our experience with Ca(*t*Bu$_2$pz)$_2$(L$_n$)[6b] suggests that the vapor pressures are very low and probably not high enough for practical use in CVD processes employing thermal source delivery. Thus, pyrazolato ligands are not likely to be as promising as other donor ligands in the search for improved volatile group 2 CVD precursors.

Experimental Section

General Considerations: All reactions were performed under argon using either glovebox or Schlenk line techniques. M[N(SiMe$_3$)$_2$]$_2$(THF)$_2$ (M = Ca, Sr, Ba),[10] *N*-*tert*-butyl-4-(*tert*-butylimino)-2-penten-2-amine (L$^{t\mathrm{Bu}}$H),[11] and 3,5-di-*tert*-butylpyrazole[29] were prepared according to reported methods. ^{1}H and ^{13}C{^{1}H} NMR spectra were obtained at 400 and 100 MHz, respectively, in [D$_8$]-toluene. Infrared spectra were obtained using Nujol as the medium. Elemental analyses were performed by Midwest Microlab, Indianapolis, IN. Melting points were obtained with a Haake-Buchler HBI digital melting point apparatus and are uncorrected.

Synthesis of [(η^2-*t*Bu$_2$pz)Ca(μ-η^5:η^2-*t*Bu$_2$pz)(μ-η^2:η^2-*t*Bu$_2$pz)Ca(η^5-L$^{t\mathrm{Bu}}$)] (1): A 100-mL Schlenk flask was charged with Ca[N(SiMe$_3$)$_2$]$_2$(THF)$_2$ (0.420 g, 0.831 mmol) and toluene (30 mL). This solution was treated with L$^{t\mathrm{Bu}}$H (0.175 g, 0.831 mmol) and was stirred at ambient temperature for 3 h. The resultant solution was then treated with *t*Bu$_2$pzH (0.150 g, 0.831 mmol) in small portions and was further stirred for 18 h. The volatile components were removed under reduced pressure and the crude material was extracted with hexane (30 mL). The hexane extract was filtered through a 2-cm pad of Celite on a coarse glass frit to afford a colorless solution. The filtrate was concentrated to a volume of 10 mL and was stored at –30 °C for 24 h to afford **1** as colorless crystals {0.06 g, 17%, based on Ca[N(SiMe$_3$)$_2$]$_2$(THF)$_2$}: m.p. 184–186 °C (dec). IR (Nujol): $\tilde{\nu}$ = 1632 (m), 1500 (m), 1250 (m), 1215 (w), 1188 (w), 1007 (w), 976 (w), 810 (w), 797 (w), 767 (w) cm^{-1}. ^{1}H NMR ([D$_8$]toluene, 23 °C): δ = 1.45, 1.40, 1.34, 1.32, 1.28, 1.13 [pyrazolato and L$^{t\mathrm{Bu}}$ C(C*H*$_3$)$_3$], 1.99, 1.98, 1.96, 1.85 (L$^{t\mathrm{Bu}}$ C*H*$_3$), 4.60, 4.44, 4.22, 4.20 (L$^{t\mathrm{Bu}}$ β-C*H*), 6.22, 6.19, 6.08, 6.04, 5.98 (pyrazolato ring β-C*H*) ppm. C$_{46}$H$_{82}$Ca$_2$N$_8$ (827.36): C 66.78, H 9.99, N 13.54; found C 66.46, H 9.89, N 13.30.

Synthesis of [Sr(μ-η^5:η^2-*t*Bu$_2$pz)(η^5-L$^{t\mathrm{Bu}}$)]$_2$ (2): In a fashion similar to the preparation of **1**, treatment of Sr[N(SiMe$_3$)$_2$]$_2$(THF)$_2$ (0.459 g, 0.831 mmol) with L$^{t\mathrm{Bu}}$H (0.175 g, 0.831 mmol), followed by *t*Bu$_2$pzH (0.150 g, 0.831 mmol) in toluene (30 mL), afforded **2** as colorless crystals upon cooling of a hot toluene solution to –30 °C {0.20 g, 50%, based on Sr[N(SiMe$_3$)$_2$]$_2$(THF)$_2$}: m.p. 245–247 °C. IR (Nujol): $\tilde{\nu}$ = 1250 (m), 1210 (m), 1186 (m), 1025 (w), 994 (w), 797 (w), 768 (w), 757 (w) cm^{-1}. ^{1}H NMR ([D$_8$]toluene, 23 °C): δ = 1.30 [s, 36 H, L$^{t\mathrm{Bu}}$ C(C*H*$_3$)$_3$], 1.47 [s, 36 H, pyrazolato C(C*H*$_3$)$_3$], 1.99 (s, 12 H, C*H*$_3$), 4.19 (s, 2 H, β-C*H*), 6.26 (s, 2 H, pyrazolato ring C*H*) ppm. ^{13}C{^{1}H} NMR ([D$_8$]toluene, 23 °C): δ = 25.21 [s, C(*C*H$_3$)], 31.57 [s, pyrazolato C(*C*H$_3$)$_3$], 32.62 [s, pyrazolato *C*(CH$_3$)$_3$], 33.01 [s, L$^{t\mathrm{Bu}}$ C(*C*H$_3$)$_3$], 54.18 [s, L$^{t\mathrm{Bu}}$ *C*(CH$_3$)$_3$], 92.00 (s, β-*C*H), 102.62 (s, pyrazolato ring *C*H), 160.21 [s, pyrazolato ring *C*C(CH$_3$)$_3$], 164.37 (s, *C*CH$_3$) ppm. C$_{48}$H$_{88}$N$_8$Sr$_2$ (952.50): C 60.53, H 9.31, N 11.76; found C 59.50, H 9.05, N 11.41. In addition to the resonances reported for **2**, 13% of Sr(η^5-L$^{t\mathrm{Bu}}$)$_2$[7b] was also observed in the ^{1}H NMR spectrum at ambient temperature in [D$_8$]toluene, and was identified by comparison of its ^{1}H NMR resonances with those of authentic material.

Synthesis of [Ba(μ-η^5:η^2-*t*Bu$_2$pz)(η^5-L$^{t\mathrm{Bu}}$)]$_2$ (3): In a fashion similar to the preparation of **2**, treatment of Ba[N(SiMe$_3$)$_2$]$_2$(THF)$_2$ (1.00 g, 1.66 mmol) with L$^{t\mathrm{Bu}}$H (0.350 g, 1.66 mmol), followed by *t*Bu$_2$pzH (0.300 g, 1.66 mmol) in toluene (30 mL), afforded **3** as a colorless crystals from toluene (0.580 g, 66%, based on Ba[N(SiMe$_3$)$_2$]$_2$(THF)$_2$): m.p. 289–291 °C. IR (Nujol): $\tilde{\nu}$ = 1247 (w), 1208 (m), 1185 (m), 1042 (w), 1023 (w), 967 (w), 793 (m), 765 (m) cm^{-1}. ^{1}H NMR ([D$_8$]toluene, 23 °C): δ = 1.30 [s, 36 H, L$^{t\mathrm{Bu}}$ C(C*H*$_3$)$_3$], 1.47 [s, 36 H, pyrazolato C(C*H*$_3$)$_3$], 2.00 (s, 12 H, C*H*$_3$), 4.18 (s, 2 H, L$^{t\mathrm{Bu}}$ β-C*H*), 6.27 (s, 2 H, pyrazolato ring C*H*) ppm. ^{13}C{^{1}H} NMR ([D$_8$]toluene, 23 °C): δ = 24.76 [s, C(*C*H$_3$)], 31.63 [s, pyrazolato C(*C*H$_3$)$_3$], 32.31 [s, pyrazolato *C*(CH$_3$)$_3$], 32.88 [s, C(*C*H$_3$)$_3$], 54.27 [s, *C*(CH$_3$)$_3$], 90.41 (s, β-*C*H), 103.25 (s, pyrazolato ring *C*H), 157.86 [s, pyrazolato ring *C*C(CH$_3$)$_3$], 162.68 (s, *C*CH$_3$) ppm. C$_{48}$H$_{88}$Ba$_2$N$_8$ (1051.94): C 54.81, H 8.43, N 10.65; found C 54.88, H 8.47, N 10.38.

X-ray Crystallography: Crystals of **1–3** were grown as described above. Diffraction data were collected with a Bruker P4/CCD diffractometer equipped with Mo radiation and a graphite monochromator at –80 °C (**1**) or at ambient temperature with the crystals mounted in glass capillaries (**2** and **3**). A sphere of data was measured at 10–20 s/frame and 0.2–0.3° between frames. The frame data were indexed and integrated with the manufacturer's SMART, SAINT, and SADABS software.[30] All structures were refined using Sheldrick's SHELX-97 software.[31] In the model for **1**, one of the *tert*-butyl groups was severely disordered and was assigned partial atoms [C(20)–C(22)]. All three structures show typically large thermal parameters in the *tert*-butyl groups. All non-hydrogen atoms were refined anisotropically and the hydrogen atom positions were calculated. Complexes **2** and **3** occupy crystallographic inversion centers. CCDC-260847 (**1**), -260848 (**2**), and -260849 (**3**) contain the supplementary crystallographic data for this paper. These data can be obtained free of charge from The Cambridge Crystallographic Data Centre via www.ccdc.cam.ac.uk/data_request/cif.

van't Hoff Analysis of 2: A 5-mm NMR tube was charged with **2** (0.0150 g, 0.0157 mmol) and [D$_8$]toluene (0.85 mL) and was sealed with a plastic cap. ^{1}H NMR spectra were recorded between 46 and

104 °C. For analysis of the data, see the text and Supporting Information.

Acknowledgments

We thank the U.S. Army Research Office (grant nos. DAAD19-01-1-0575 and W911NF-04-1-0332) for generous support of this research.

[1] For recent reviews of group 2 complexes and their applications in CVD, see: a) T. P. Hanusa, *Organometallics* **2002**, *21*, 2559–2571; b) J. S. Matthews, W. S. Rees, Jr., *Adv. Inorg. Chem.* **2000**, *50*, 173–192; c) W. A. Wojtczak, P. F. Pfleig, M. J. Hampden-Smith, *Adv. Organomet. Chem.* **1996**, *40*, 215–340; d) D. Schulz, T. J. Marks, *Adv. Mater.* **1994**, *6*, 719–730; e) A. R. Barron, W. S. Rees, Jr., *Adv. Mater. Opt. Electron.* **1993**, *2*, 271–288.

[2] Leading references to group 2 CVD precursors with cyclopentadienyl ligands: a) T. Hatanpää, M. Vehkamäki, I. Mutikainen, J. Kansikas, M. Ritala, M. Leskelä, *J. Chem. Soc., Dalton Trans.* **2004**, 1181–1188; b) M. Vehkamäki, T. Hänninen, M. Ritala, M. Leskelä, T. Sajavaara, E. Rauhala, J. Keinonen, *Chem. Vap. Deposition* **2001**, *7*, 75–80; c) M. Vehkamäki, T. Hänninen, M. Ritala, M. Leskelä, *Electrochem. Solid-State Lett.* **1999**, *2*, 504–506.

[3] Recent selected references to group 2 CVD precursors with β-diketonato and β-ketoiminato ligands: a) A. Kosola, M. Putkonen, L.-S. Johansson, L. Niinistö, *Appl. Surf. Sci.* **2003**, *211*, 102–112; b) V. Sannila, J. Ihanus, M. Ritala, M. Leskelä, *Chem. Vap. Deposition* **1998**, *4*, 227–233; c) A. R. Teren, J. A. Belot, N. L. Edleman, T. J. Marks, B. W. Wessels, *Chem. Vap. Deposition* **2000**, *6*, 175–177; d) D. B. Studebaker, D. A. Neumayer, B. J. Hinds, C. L. Stern, T. J. Marks, *Inorg. Chem.* **2000**, *39*, 3148–3157; e) J. A. Belot, D. A. Neumayer, C. J. Reedy, D. B. Studebaker, B. J. Hinds, C. L. Stern, T. J. Marks, *Chem. Mater.* **1997**, *9*, 1638–1648.

[4] For selected, leading references, see: a) X. He, B. C. Noll, A. Beatty, R. E. Mulvey, K. W. Henderson, *J. Am. Chem. Soc.* **2004**, *126*, 7444–7445; b) S. Harder, S. Müller, E. Hübner, *Organometallics* **2004**, *23*, 178–183; c) M. S. Hill, P. B. Hitchcock, *Chem. Commun.* **2003**, 1758–1759; d) F. Feil, S. Harder, *Macromolecules* **2003**, *36*, 3446–3448; e) M. H. Chisholm, J. Gallucci, K. Phomphrai, *Chem. Commun.* **2003**, 48–49; f) F. Feil, S. Harder, *Eur. J. Inorg. Chem.* **2003**, 3401–3408; g) S. Harder, F. Feil, *Organometallics* **2002**, *21*, 2268–2274; h) S. Harder, F. Feil, A. Weeber, *Organometallics* **2001**, *20*, 1044–1046; i) F. Feil, S. Harder, *Organometallics* **2000**, *19*, 5010–5015.

[5] a) S. Harder, *Angew. Chem. Int. Ed.* **2003**, *42*, 3430–3434; b) S. Harder, *Organometallics* **2002**, *21*, 3782–3787.

[6] a) D. Pfeiffer, M. J. Heeg, C. H. Winter, *Angew. Chem. Int. Ed.* **1998**, *37*, 2517–2519; b) D. Pfeiffer, M. J. Heeg, C. H. Winter, *Inorg. Chem.* **2000**, *39*, 2377–2384.

[7] a) H. M. El-Kaderi, M. J. Heeg, C. H. Winter, *Organometallics* **2004**, *23*, 3488–3495; b) H. M. El-Kaderi, A. Xia, M. J. Heeg, C. H. Winter, *Organometallics* **2004**, *23*, 4995–5002.

[8] For reviews of pyrazolato complexes, see: a) F. Nief, *Eur. J. Inorg. Chem.* **2001**, 891–904; b) J. E. Cosgriff, G. B. Deacon, *Angew. Chem. Int. Ed.* **1998**, *37*, 286–287; c) G. La Monica, G. A. Ardizzoia, *Progr. Inorg. Chem.* **1997**, *46*, 151–238; d) A. P. Sadimenko, S. S. Basson, *Coord. Chem. Rev.* **1996**, *147*, 247–297; e) S. Trofimenko, *Progr. Inorg. Chem.* **1986**, *34*, 115–210; f) S. Trofimenko, *Chem. Rev.* **1972**, *72*, 497–508.

[9] a) A. Steiner, G. T. Lawson, B. Walfort, D. Leusser, D. Stalke, *J. Chem. Soc., Dalton Trans.* **2001**, 219–221; b) A. Steiner, D. Stalke, *Inorg. Chem.* **1995**, *34*, 4846–4853; c) J. Hitzbleck, A. Y. O'Brien, C. M. Forsyth, G. B. Deacon, K. Ruhlandt-Senge, *Chem. Eur. J.* **2004**, *10*, 3315–3323; d) J. Hitzbleck, G. B. Deacon, K. Ruhlandt-Senge, *Angew. Chem. Int. Ed.* **2004**, *43*, 5218–5220.

[10] a) B. A. Vaartstra, J. C. Huffman, W. E. Streib, K. G. Caulton, *Inorg. Chem.* **1991**, *30*, 121–125; b) M. Westerhausen, *Inorg. Chem.* **1991**, *30*, 96–101.

[11] a) N. Kuhn, J. Fahl, S. Fuchs, M. Steimann, G. Henkel, A. H. Maulitz, *Z. Anorg. Allg. Chem.* **1999**, 2108–2114; b) N. Kuhn, H. Lanfermann, P. Schmitz, *Liebigs Ann. Chem.* **1987**, 727–728.

[12] R. A. Williams, T. P. Hanusa, J. C. Huffman, *Organometallics* **1990**, *9*, 1128–1134.

[13] J. R. Perera, M. J. Heeg, H. B. Schlegel, C. H. Winter, *J. Am. Chem. Soc.* **1999**, *121*, 4536–4537.

[14] F. Weber, H. Sitzmann, M. Schultz, C. D. Sofield, R. A. Andersen, *Organometallics* **2002**, *21*, 3139–3146.

[15] For example, see: I. N. Levine, *Physical Chemistry*, 3rd ed., McGraw-Hill, New York, **1988**, pp. 177–180.

[16] a) A. G. Avent, M. R. Crimmin, M. S. Hill, P. B Hitchcock, *Dalton Trans.* **2005**, 278–284; b) M. R. Crimmin, I. J. Casely, M. S. Hill, *J. Am. Chem. Soc.* **2005**, *127*, 2042–2043; c) A. G. Avent, M. R. Crimmin, M. S. Hill, P. B. Hitchcock, *Dalton Trans.* **2004**, 3166–3168; d) M. S. Hill, P. B. Hitchcock, *Chem. Commun.* **2003**, 1758–1759.

[17] M. H. Chisholm, J. C. Galucci, K. Phomphrai, *Inorg. Chem.* **2004**, *43*, 6717–6725.

[18] W. Clegg, S. J. Coles, E. K. Cope, F. S. Mair, *Angew. Chem. Int. Ed.* **1998**, *37*, 796–798.

[19] a) L. Bourget-Merle, M. F. Lappert, J. R. Severn, *Chem. Rev.* **2002**, *102*, 3031–3066.

[20] a) G. B. Nikiforov, H. W. Roesky, D. Vidovic, J. Magull, *J. Mol. Struct.* **2003**, *656*, 155–160; b) P. B. Hitchcock, M. F. Lappert, D.-S. Liu, *J. Chem. Soc., Chem. Commun.* **1994**, 2637–2638; c) M. Rahim, M. J. Taylor, S. Xin, S. Collins, *Organometallics* **1998**, *17*, 1315–1323; d) L. Kakaliou, W. J. Scanlon, B. Qian, S. W. Baek, M. R. Smith III, D. H. Motry, *Inorg. Chem.* **1999**, *38*, 5964–5977; e) R. Vollmerhaus, M. Rahim, R. Tomaszewski, S. Xin, N. J. Taylor, S. Collins, *Organometallics* **2000**, *19*, 2161–2169.

[21] G. B. Deacon, C. M. Forsyth, A. Gitlits, B. W. Skelton, A. H. White, *Dalton Trans.* **2004**, *8*, 1239–1247.

[22] Ionic radii were taken from: N. N. Greenwood, A. Earnshaw, *Chemistry of the Elements*, 2nd ed., Butterworth-Heinemann, Oxford, **1997**, pp. 111, 1233.

[23] G. B. Deacon, A. Gitlits, P. W. Roesky, M. R. Bürgstein, K. C. Lim, B. W. Skelton, A. H. White, *Chem. Eur. J.* **2001**, *7*, 127–138.

[24] M. J. McCormick, S. C. Sockwell, C. E. H. Davis, T. P. Hanusa, J. C. Huffman, *Organometallics* **1989**, *8*, 2044–2049.

[25] D. J. Burkey, E. K. Alexander, T. P. Hanusa, *Organometallics* **1994**, *13*, 2773–2786.

[26] A. Weeber, S. Harder, H. H. Brintzinger, K. Knoll, *Organometallics* **2000**, *19*, 1325–1332.

[27] H. Sitzmann, F. Weber, M. D. Walter, G. Wolmershäuser, *Organometallics* **2003**, *22*, 1931–1936.

[28] a) J. S. Alexander, K. Ruhlandt-Senge, *Eur. J. Inorg. Chem.* **2002**, 2761–2764; b) M. Westerhausen, *Angew. Chem. Int. Ed.* **2001**, *40*, 2975–2977.

[29] J. Elguéro, E. Gonzalez, R. Jacquier, *Bull. Soc. Chim. Fr.* **1968**, 707.

[30] *APEX II*, *SMART*, *SAINT*, and *SADABS* collection and processing programs are distributed by Bruker AXS, Inc., Madison, Wisconsin, USA.

[31] G. Sheldrick, SHELX-97, University of Göttingen, Germany, **1997**.

Received January 26, 2005

